

I-1. PROJECT RESEARCHES

Project 6

PR6 Enhancement of research methods for material irradiation and defect analysis

A. Kinomura

*Institute for Integrated Radiation and Nuclear Science,
Kyoto University*

OBJECTIVES: Irradiation facilities of high-energy particles for neutrons (Material Controlled irradiation Facility), ions (e.g., Heavy ion irradiation facility) and electrons (Temperature-controlled irradiation facilities of KUR-LINAC) have been extensively developed at the Institute for Integrated Radiation and Nuclear Science. The developed facilities have been in operation and opened for joint research projects. One of the objectives of this project is to further improve or optimize irradiation facilities for advanced irradiation experiments.

As characterization techniques for irradiated materials, a slow positron-beam system and a focused ion beam system have been developed and introduced, respectively, in addition to previous characterization facilities such as an electron microscope, an electron-spin-resonance spectrometer, a bulk positron annihilation spectrometer and a thermal desorption spectrometer. Another objective is to introduce new techniques or reconsider analytical methods of previously used characterization techniques.

Based on these two objectives, we expect the enhancement of previous studies and the attraction of new users for the joint research program.

The allotted research subjects (ARS) and co-researchers are listed below. The titles of research subjects are taken from the individual reports.

ARS-1:

Study to improve transport and measurement performance of a slow positron beamline (A. Kinomura et al.)

ARS-2:

Doping effect of Re, Mo, Ta on electron irradiation induced defects in W (T. Toyama et al.)

ARS-3:

Change in the Positron Annihilation Lifetime of Electron-irradiated F82H by Hydrogen Charging 2 (K. Sato et al.)

ARS-4:

Gamma-ray induced light emission from GaN single crystal wafer (T. Nakamura et al.)

ARS-5:

Irradiation technique for study on corrosion resistance of fusion divertor materials to liquid metal during irradiation (M. Akiyoshi et al.)

ARS-6:

Change of free volume in hydrogenated DLC film by the irradiation of soft X-rays (K. Kanda et al.)

ARS-7

Positron annihilation spectroscopy on diamond-like carbon films (S. Nakao et al.)

RESULTS:

In ARS-1, the brightness enhancement system of the

KUR slow positron beamline was evaluated and the brightness enhancement values of 5.6 - 8.5 were obtained from phosphor screen images of microchannel plates. The actual samples were measured by positron annihilation lifetime spectroscopy using the KUR slow positron beam.

In ARS-2, electron-irradiation to W or W-5%Re (in weight %) was performed. After electron irradiation, the average lifetime increased, showing positron trapping to vacancy type defects. In contrast, the average lifetime for W 5%Re remained relatively short compared with the other alloys, suggesting that the formation of irradiation induced defects was suppressed.

In ARS-3, positron lifetimes of the number of hydrogen atoms trapped at vacancy clusters in electron-irradiated F82H were estimated and compared with the results of positron annihilation lifetime spectroscopy. The decrease in the positron lifetime per additional hydrogen atom is approximately 5 ps for 4 hydrogen atoms or less, and approximately 2 ps for 5 hydrogen atoms or more. However, the positron lifetime is almost constant when V5 contains 7 and 8 hydrogen atoms.

In ARS-4, as-grown and gamma-ray irradiated GaN single crystal wafers irradiated at room temperature with gamma-rays of a cobalt-60 source. One end of the optical fiber cable was set on the front face of the GaN placed near the Co source and was led to the analysis room with the spectrometer. The emission characteristics of as-grown GaN and gamma-irradiated GaN were compared.

In ARS-5, irradiation techniques for study on corrosion resistance of fusion divertor materials to liquid metal during irradiation have been developed in this research subject. However, the planned experiments were not performed this year due to the limitation of the sample preparation period.

In ARS-6, The irradiation of soft X-rays to the H-DLC film was carried out at BL06 of the NewSUBARU synchrotron facility. In Doppler broadening measurements of the irradiated samples, the W parameter decreased linearly with increasing of the S parameter. This indicated that the same types of positron trapping sites are present.

In ARS-7, positron annihilation spectroscopy were performed for type-IV (a-C:H) and type-VI (PLC) films deposited by plasma-based ion implantation (PBII). The S-parameters of carbon layer significantly decrease to ~0.47 for both a-C:H and PLC films after annealed at 800°C. However, a-C:H films only indicate the decrease in S-parameters at shallower region of the films.

SUMMARY: Several new irradiation (electron-beam and gamma-rays) and analytical (slow beam and conventional positron measurements) techniques for various materials have been developed and demonstrated for the objectives of this project. Such studies may enhance developments of new techniques and materials in various scientific fields.

PR6-1 Study to improve transport and measurement performance of a slow positron beamline

A. Kinomura, N. Oshima¹, A. Uedono² and A. Yabuuchi

*Institute for Integrated Radiation and Nuclear Science,
Kyoto University*

¹*National Institute of Advanced Industrial Science and
Technology (AIST)*

²*University of Tsukuba*

INTRODUCTION: Positron annihilation spectroscopy is an important analytical method to detect vacancy-type defects and vacant spaces of materials. Energy-variable mono-energetic positron beams (slow positron beams) are essential to perform depth-dependent positron annihilation spectroscopy of surface layers such as ion-implanted layers or thin films formed on substrates. Intense positron sources are necessary to obtain slow positron beams for practical use. In general, positron sources based on pair creation can provide higher intensity than radioisotope-based positron sources. A positron source using pair-creation by gamma-rays from a nuclear reactor have been developed by using Kyoto University research Reactor (KUR) to obtain a slow positron beam for materials analysis. In the KUR slow positron beamline, the source size (converter and moderator assembly) is approximately 30 mm in diameter. For typical sample sizes of materials analysis (≤ 10 mm), it is necessary to reduce beam sizes efficiently while keeping beam intensity as high as possible. For this purpose, a brightness enhancement system has been developed for the KUR slow positron beamline [1]. In addition, measurement systems for positron annihilation lifetime spectroscopy have been optimized in this study.

EXPERIMENTS: The brightness enhancement system of the KUR slow positron beam system has been evaluated in terms of the spot size and the beam intensity. A single-crystalline Ni thin film annealed in vacuum at 750 °C for 1h was used as a re-moderator of the brightness enhancement system. The Ni re-moderator film was cleaned by thermally excited hydrogen atoms after installation in vacuum to remove contamination during handling in air.

The spot sizes and the intensities of the brightness enhanced beams was checked for previously obtained experimental data. In particular, the data sets of the spot images were carefully investigated again by appropriate data treatments. Brightness values were recalculated from the obtained spot sizes as well as the previously measured beam intensities

RESULTS: Beam-spot images were obtained by phosphor screens on microchannel plates (MCP's). The brightness enhancement system was optimized by observing the spot images on the MCP screen positioned at the focal point of the lens. The beam profiles at individual MCP screens were taken using a digital single-lens reflex camera with a CMOS CCD (charge coupled device) image sensor as digital photographs. To avoid unnecessary data processing in the camera, a RAW-mode (a raw-data mode without data processing)

was selected for this experiment. Parameters of image acquisition were appropriately selected to keep the linearity of the combination of the MCP and the image sensor (CCD).

Figure 1 shows the normalized horizontal (x-direction) and vertical (y-direction) intensity profiles of the beam spots before and after the brightness enhancement. The distribution in the beam spot were different for horizontal and vertical directions as shown in fig. 1. One of the reasons is that the beam shape at the entrance of the beamline is not circular. We believe that the original beam (i.e., circular beam) extracted from the source was cut several times by the walls of vacuum ducts during beam transportation. We evaluated spot size as a full-width at half-maximum (FWHM) value for horizontal and vertical directions.

The brightness enhancement experiments were performed at acceleration energies of 5.0 – 6.5 keV. The original beam size of ~ 10 mm was focused to ~ 1.5 mm. Calculated demagnification factors were approximately 1/6.4 – 1/7.4. The efficiencies of the re-moderator were measured to be 2.3 – 3.8% by gamma-ray intensities measured from the MCPs placed before and after the brightness enhancement system. Based on these measured values, the brightness enhancement values were calculated to be 5.6 - 8.5.

The performance of the positron pulsing system was confirmed last year [2] and the actual samples have been successfully measured by positron annihilation lifetime spectroscopy.

In summary, transport and measurement performance of the KUR slow positron system was evaluated with a positron beam during the KUR operation. The brightness enhancement system and positron pulsing system were confirmed to be effective.

REFERENCES:

- [1] Y. Kuzuya et al. J. Phys. Conf. Series 791 (2017) 012012.
- [2] M. Nakajima et al. Rev. Sci. Instrum. 91 (2020) 125109.

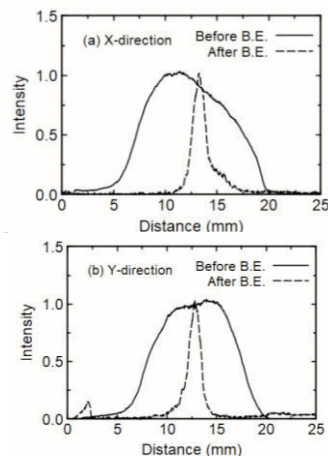


Fig. 1 Beam spot profiles for x and y directions, respectively, before and after brightness enhancement.

PR6-2 Doping effect of Re, Mo, Ta on electron-irradiation induced defects in W

T. Toyama¹, Y. Hatano², T. Suzudo¹, C. Zhao¹, K. Inoue¹, A. Yabuuchi³, A. Kinomura³, Y. Nagai¹

¹Institute for Materials Research, Tohoku University

²Organization for Promotion of Research, University of Toyama

³Institute for Integrated Radiation and Nuclear Science, Kyoto University

INTRODUCTION: Development of the plasma-facing materials for fusion reactors is in progress over the world. Tungsten (W) is a primary candidate material due to its high melting point, high sputtering resistance to energetic particles, and the very low solubility of hydrogen isotopes which is a notable advantage in reducing tritium (T) retention. However, recent studies have reported that neutron-irradiation and ion-irradiation cause significant enhancement of hydrogen isotope retention in W, due to hydrogen trapping at irradiation-induced defects such as vacancies, vacancy clusters, and dislocation loops. Recently it was found that the addition of rhenium (Re) to W drastically reduces the hydrogen isotope accumulation [1]. As a mechanism for this, quantum chemical calculation has been performed [2]; it is suggested that Re is strongly bound to interstitial atoms, so that recombination of interstitial atoms and vacancies is promoted, and the formation of vacancy-type defects that become hydrogen capture sites is suppressed. However, no experimental studies on this have been obtained. In this study, we performed electron-irradiation to introduce only a simple Frenkel pair to W or W-Re alloy. The effect of Re addition on the defect formation is investigated by the positron annihilation method. In addition, the effect of Mo and Ta is investigated.

EXPERIMENTS: Electron-irradiation to pure W, W-5%Re (in weight %), W-1.5%Mo, and W-5%Ta was performed at LINAC at KUR at 8 MeV, at temperature of < 100 °C to the fluence of $\sim 4 \times 10^{23}$ e⁻/m². Positron annihilation measurements (lifetime measurement and coincidence Doppler broadening measurement) were performed. Three-dimensional atom probe (3D-AP) observation was also performed.

RESULTS: Figure 1 shows results of average positron lifetime before and after electron-irradiation for the samples. In pure W, the average lifetime was about 120 ps before electron-irradiation, which is close to the value in W bulk. After electron-irradiation, the average lifetime increased, showing positron trapping to vacancy-type defects induced by electron-irradiation. In W-1.5%Mo and W-5%Ta alloys, the trends were almost similar to that for pure W, indicating that the effect of these elements on the formation of irradiation-induced defects are not significant. In contrast, the average lifetime for W-5%Re remained relatively short compared with the other alloys, suggesting that the formation of irradiation-induced defects was suppressed. The possible candidate for positron trapping site for W-5%Re after irradiation could be dis-

locations in which positron life-time value may be shorter than mono-vacancy. Other candidate could be vacancy-Re complexes, however, positron lifetime value at vacancy-Re complex might be almost same as at mono-vacancy in W because Re and W are the “neighborhood” in the periodic table. Figure 2 shows the atom maps of Re obtained by 3D-AP. It was revealed that no Re clusters were formed after electron-irradiation. The kinetics of the irradiation-induced defects, i.e. interstitials and vacancies in W-Re alloy is now being simulated with quantum chemical calculation, which would make a direct comparison with the present results to understand the dynamic behavior of defects and solutes under irradiation.

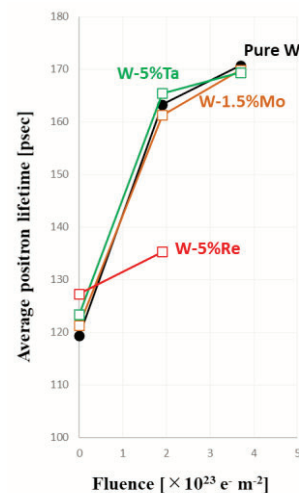


Fig. 1. Average positron lifetime before and after electron-irradiation.



Fig. 2. Atom maps of Re for W-5%Re alloy before and after electron-irradiation.

REFERENCES:

- [1] Y. Hatano et al., Nucl. Mater. Energy 9 (2016) 93.
- [2] T. Suzudo, A. Hasegawa, Sci. Rep. 6 (2016) 36738.

PR6-3 Change in the Positron Annihilation Lifetime of Electron-irradiated F82H by Hydrogen Charging 2

K. Sato, M. Hirabaru, Y. Kondo, M. Ohta, Q. Xu¹, A. Yabuuchi¹, A. Kinomura¹

Graduate School of Science and Engineering, Kagoshima University

¹*Institute for Integrated Radiation and Nuclear Science, Kyoto University*

INTRODUCTION: The structural materials of spallation neutron sources (SNS) cause more serious irradiation damage than fission reactors due to high-energy protons or spallation neutrons and the formation of extremely larger amount of gas atoms by nuclear transmutation [1, 2]. Therefore, irradiation resistance is required. Reduced activation ferritic/martensitic steel F82H, one of the candidates for fusion reactor structural materials, has good thermal and mechanical properties [3]. Using this steel, many researchers have investigated the effect of He or H on its microstructural evolution [4–6]. The increase in hydrogen retention caused by the interaction with defects has an influence on the mechanical properties of structural materials [7, 8]. Vacancy-type defects are detected well by positron annihilation spectroscopy (PAS). Sato et al. determined the change in the positron annihilation lifetime (PAL) through experiments and simulations [9]. Comparison and estimation of the number of hydrogen atoms trapped at single vacancies in electron-irradiated tungsten by PAS were performed [9]. In this study, to estimate the quantity of hydrogen atoms trapped at vacancy clusters in electron-irradiated F82H, we calculated the PAL of vacancy clusters containing the hydrogen atoms in Fe.

CALCULATION METHODS: The Schrödinger equation of a positron wave function was calculated using the method developed by Puska and Nieminen [10]. The electron density was constructed by the superposition of the atomic wave function provided by Herman and Skillman [11] for core electrons (1s, 2s, 2p, 3s, and 3p), and was obtained using the VASP code [12, 13] for valence electrons (3d, and 4s). The same simulation method as in previous works [9, 14] was used in this study. For the same number of hydrogen atoms trapped at V_5 , all configurations were calculated by VASP to obtain the total energy of the model lattice. The PAL was calculated using the configuration with the lowest total energy.

RESULTS: Table 1 shows the calculated PAL of V_5H_n complexes in Fe. The PAL decreases with increasing number of hydrogen atoms. The decrease in the PAL per additional hydrogen atom is approximately 5 ps for 4 hydrogen atoms or less, and approximately 2 ps for 5 hydrogen atoms or more. However, the PAL is almost constant when V_5 contains 7 and 8 hydrogen atoms. This trend agrees with those in previous studies [9, 15]. The number of hydrogen atoms trapped at vacancy clusters

during hydrogen charging was estimated using the same method as in [9]. When we theoretically estimated the number of hydrogen atoms trapped at vacancy clusters under cathodic electrolysis hydrogen charging according to Oriani's local equilibrium theory, the value was 14.1. On the other hand, compared between the calculated and experimental results, each V_5 contains 4 hydrogen atoms. This value is much lower than the theoretical value mentioned above. Since samples are kept at ambient temperature for 5 minutes after hydrogen charging, we also discussed whether hydrogen atoms can be de-trapped during 5 minutes. The difference between experimental results and theory cannot be explained by the annealing at ambient temperature.

Table 1. Calculated PAL of V_5H_n complexes vs the number of hydrogen atoms trapped at V_5 (n) in Fe.

Number of hydrogen atoms trapped at V_5 .	Positron annihilation lifetime (ps)
0	247
1	242
2	239
3	234
4	228
5	226
6	224
7	222
8	222
10	218
12	214
14	208

REFERENCES:

- [1] Y. Dai, G.S. Bauer, *J. Nucl. Mater.* 296 (2001) 43.
- [2] Y. Dai et al., *J. Nucl. Mater.* 343 (2005) 33.
- [3] M. Tamura et al., *J. Nucl. Mater.* 141–143 (1986) 1067.
- [4] X. Jia, Y. Dai, *J. Nucl. Mater.* 318 (2003) 207.
- [5] Z. Tong, Y. Dai, *J. Nucl. Mater.* 385 (2009) 258.
- [6] Z. Tong, Y. Dai, *T J. Nucl. Mater.* 398 (2010) 43.
- [7] H.K. Birnbaum, P. Sofronis, *Mater. Sci. Eng. A* 176 (1994) 191.
- [8] M. Nagumo et al., *Metall. Mater. Trans. A* 32 (2001) 339.
- [9] K. Sato et al., *J. Nucl. Mater.* 496 (2017) 9.
- [10] M.J. Puska, R.M. Nieminen, *J. Phys. F* 13 (1983) 333.
- [11] F. Herman, S. Skillman, *Atomic Structure Calculations*, Prentice Hall, Inc., Englewood Cliffs, New Jersey, 1963.
- [12] G. Kresse, J. Hafner, *Phys. Rev. B* 47 (1993) 558.
- [13] G. Kresse, J. Furthmüller, *Phys. Rev. B* 54 (1996) 11169.
- [14] K. Sato, et al., *Phys. Rev. B* 75 (2007) 094109.
- [15] B.L. Shivachev et al., *J. Nucl. Mater.* 306 (2002) 105.

T. Nakamura¹, T. Nishimura¹, K. Kuriyama¹, Atsushi Kinomura²

¹Research Center of Ion Beam Technology, Hosei University, Koganei, Tokyo 184-8584, Japan

²Institute for Integrated Radiation and Nuclear Science, Kyoto University, Kumatori, Osaka 590-0494, Japan

INTRODUCTION: Emission characteristics for native and radiation induced defects of wide-gap semiconductors such as GaN have been studied by cathode-luminescence using an electron beam and photoluminescence using a UV laser. The possibility in luminescence excited by gamma rays for GaN is an interesting issue. This is because GaN can be used as an application for a gamma ray detector. Furthermore, examining the defects caused by various radiations on GaN is important when assuming its use under the space environment. In our previous study [1, 2], we reported that the energy levels relating to nitrogen vacancy (VN) and gallium vacancy (VGa) were induced by neutron and proton irradiated GaN. The neutron irradiation has been used as the neutron transmutation doping into semiconductors such as GaAs [3], GaP [4], and GaN [5]. We have also reported that the high resistive ZnO bulk single crystals became low resistive due to the Zn interstitials induced by gamma irradiation [6]. Therefore, to survey the radiation effect of gamma ray alone is meaningful.

EXPERIMENTS: As-grown and gamma-ray irradiated GaN single crystal wafers with thicknesses of 250 ~ 750 nm were used for the present study. The crystals were irradiated at room temperature with gamma-rays of 1.17 and 1.33 MeV from a cobalt-60 source of Institute for Integrated Radiation and Nuclear Science, Kyoto University. One end of the optical fiber cable was set on the front face of GaN placed near the Co source and was led to the analysis room with the spectrometer. Part of as-grown GaN was pre-irradiated with an absorption dose rate of 1.771 KGy/h. Total gamma-ray dose for the present study was 990 kGy. The emission characteristics of as-grown GaN and gamma-irradiated GaN were compared. Finally, we compared the photo emission induced by gamma rays with the photoluminescence using a He-Cd laser.

RESULTS: Figures 1(a) and 1(b) show the absorption dose rate dependence of the gamma-ray induced photo emission spectra and the absorption dose rate dependence of the integrated emission intensity, respectively. The film thickness of as-grown GaN single crystal wafer used for the measurement is 250 nm. The integrated intensity on the vertical axis is the integrated value of the entire measurement wavelength range of the emission spectrum. As the absorbed dose rate of gamma rays increases, the emission intensity increases, and the integrated emission intensity increases almost in proportion to the absorption dose rate of gamma-ray. However, the emission peak position near 600 nm did not change due to the difference

in absorbed dose rate. The possible excitation mechanism in gamma-ray induced light emission is Compton electrons produced by gamma-ray irradiation.

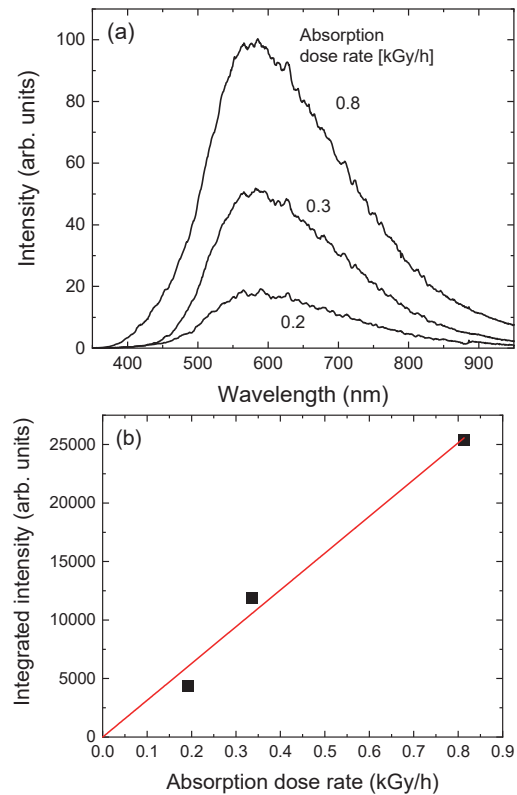


Fig. 1. (a) Absorption dose rate dependence of the gamma-ray induced photo emission spectra from the as-grown GaN single crystal wafer. (b) Absorption dose rate dependence of the integrated emission intensity for the as-grown GaN single crystal wafer.

Part of this research was published in Applied Physics Letters 118, 032106 (2021).

REFERENCES:

- [1] K. Kuriyama, M. Ooi, A. Onoue, K. Kushida, M. Okada and Q. Xu, Appl. Phys. Lett. **88** (2006) 132109.
- [2] T. Nakamura, N. Nishikata, K. Kamioka, K. Kuriyama and K. Kushida, Nucl. Instrum. Method Phys. Res. B **371** (2016) 251.
- [3] M. Satoh, K. Kuriyama and T. Kawakubo, J. Appl. Phys. **67** (1990) 3542.
- [4] K. Kuriyama, Y. Miyamoto, T. Koyama, O. Ogawa and M. Okada, J. Appl. Phys. **86** (1999) 2352
- [5] K. Kuriyama, T. Tokumasu, J. Takahashi, H. Kondo and M. Okada, Appl. Phys. Lett. **80** (2002) 3328.
- [6] J. Tashiro, Y. Torita, T. Nishimura, K. Kuriyama, K. Kushida, Q. Xu and A. Kinomura, Solid State Commun. **292** (2019) 24.

PR6-5 Change of free volume in hydrogenated DLC film by the irradiation of soft X-rays

K. Kanda, F. Hori¹, A. Yabuuchi² and A. Kinomura²

Laboratory of Advanced Science and Technology for Industry, University of Hyogo

¹Department of Materials Science, Osaka Prefecture University

²Institute for Integrated Radiation and Nuclear Science, Kyoto University

INTRODUCTION: Diamond-like carbon (DLC) film generally has a very strong tolerance of soft X-ray irradiation. However, highly hydrogenated DLC (H-DLC) film with a hydrogen content greater than 40 at.% was reported to be modified by the irradiation of soft X-rays [1]. Soft X-ray irradiation against H-DLC film decreases the film volume and hydrogen content and increases hardness. The density of the H-DLC film was reported to increase dramatically from 1.25 g/cm³ before irradiation to 1.40 g/cm³ after the irradiation of soft X-rays with 200 mA·h. However, how the free volume in DLC films is changed by soft X-ray irradiation has not been investigated at all. In this study, we observed the dependence of the free volume in the H-DLC film on the dose of soft X-ray irradiation by Positron lifetime spectroscopy (PAS) measurement using a slow positron beam, and discussed the structural change of the H-DLC film caused by hydrogen desorption upon soft X-ray irradiation.

EXPERIMENTS: H-DLC film was deposited on Si wafers by using an amplitude-modulated radio-frequency plasma-enhanced chemical vapor deposition method. (Nippon ITF Co.) The desired film thickness was 200-nm-thick. The hydrogen content of H-DLC film was estimated to be ≈50 at.%.

The irradiation of soft X-rays to the H-DLC film was carried out at BL06 of the NewSUBARU synchrotron facility [2]. The synchrotron radiation (SR) at the BL06 sample stage had a continuous spectrum from infrared to soft X-rays, lower than 1 keV. An SR dose [mA·h] is derived from the product of the ring current [mA] and exposure time [h].

Positron lifetime spectroscopy (PAS) measurement was performed at the slow positron beam system (B-1) at Kyoto University research Reactor (KUR). Doppler broadening profiles of annihilation γ -rays were obtained using a Ge detector for each positron energy. The low and high momentum parts of spectra were characterized by the S and W parameters. S and W parameters as a function of energy were measured in the range of 0 - 30 keV. Positron annihilation lifetime spectroscopy (PALS) was performed at an energy of 2 keV, corresponding to the DLC film on Si. A Kapton (polyimide) film was measured before and after measurements of the DLC samples as a control sample. Obtained lifetime spectra were analyzed by the PALSfit code assuming one-lifetime component.

RESULTS: Figure 1 shows the SR dose-dependence of positron annihilation lifetime. The positron annihilation

lifetime of the H-DLC film before irradiation was 0.41 ns and it increased to ≈0.44 ns rapidly at an SR dose of less than 500 mA·h. However, at an SR dose above 500 mA·h, the positron annihilation lifetime was approximately constant at ≈0.44. An increase in positron annihilation lifetime indicates an expansion of free volume in H-DLC film. That is to say, the desorption of hydrogen caused by the irradiation of soft X-rays increases the film density but increases the volume of the voids.

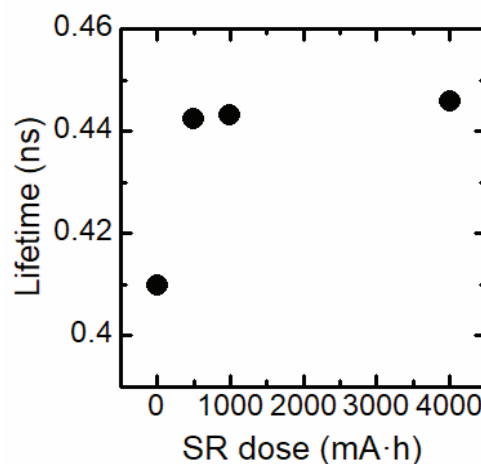


Fig. 1 The SR dose-dependence of positron annihilation life-time.

The W parameters were plotted as a function of the S parameter in Fig. 2. The W parameter decreased linearly with increasing of the S parameter. This indicated that the same types of positron trapping sites are present. In other words, different types of vacancies were not created by the desorption of hydrogen due to the SR irradiation.

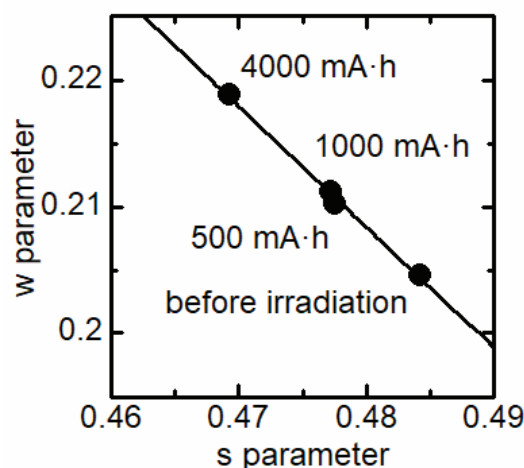


Fig. 2 The core annihilation parameter W versus the valence parameter S , in H-DLC films before and after SR irradiation.

REFERENCES:

- [1] K. Kanda *et al.*, *Sen. Mater.*, 29 (2017) 817-826.
- [2] J. Taniguchi *et al.*, *Jpn. J. Appl. Phys.*, 41 (2002) 4304-4306.

S. Nakao, X. Qu¹, A. Yabuuchi¹ and A. Kinomura¹

Structure Materials Research Institute, National Institute of Advanced Industrial Science and Technology
¹Institute for Integrated Radiation and Nuclear Science, Kyoto University

INTRODUCTION: Diamond-like carbon (DLC) films have attracted much attention because of their excellent mechanical properties. However, the properties strongly depend on the microstructure of the films which is varied by the deposition conditions and methods. Recently, DLC or carbon graphs are categorized from type I to VI, which includes graphite-like carbon (GLC) and polymer-like carbon (PLC).

The thermal stability of the films is of importance for practical applications. However, the thermal stability is not always enough at high temperature. It is considered that the degradation of the properties should be caused by the changes of the microstructure at high temperature. The structural changes may be related to hydrogen (H) desorption and creation of defects at high temperature. Many studies have been carried out on the thermal stability of DLC films. However, the principal phenomena, such as defect behavior, are not always clear. Therefore, to make clear the behavior of defects is necessary for every type of DLC films (type I to VI) because of different microstructure and hydrogen content. The positron annihilation spectroscopy (PAS) is one of the useful methods to clarify the defect behavior of materials. The aim of this study is to examine the relationship between the thermal stability and the behavior of defects in several types of DLC films by PAS and thermal desorption (TDS) method.

In a previous report [1,2], the films of type I, III, IV, V and VI were examined by TDS measurement from room temperature (RT) to 800°C and it was found that H desorption clearly started at ~600°C for a-C:H (type IV) films and at ~400°C for PLC (type VI) films. The results suggested that defects may be created due to H desorption by annealing and the behavior may play important role for the durability of the films. Several types of DLC and carbon films were also examined by PAS measurement [3,4]. The results showed that the situation of the defect in the type III – V films may be similar among as-grown films. However, the changes of S-parameters by thermal annealing might be slightly different depending on preparation conditions, such as source gases. In this study, a-C:H and PLC films are annealed every 200°C up to 800°C and examined by PAS measurement.

EXPERIMENTS: Samples for PAS measurement were type IV (a-C:H) and VI (PLC) films which were deposited by plasma-based ion implantation (PBII) under the different conditions. The details on the PBII system were reported elsewhere [5]. Si wafer was used as substrate. The S-parameter was obtained at different positron energies ranging from 0 to 30 keV.

RESULTS: Figure 1 shows the change in S-parameter against positron energy obtained from the PAS spectra of the samples, (a) a-C:H and (b) PLC films, at different annealing temperature. The S-parameters of ~0.49 at less than 5keV and ~0.52 at higher energies correspond to carbon film layer and Si substrate, respectively. The S-parameters of carbon layer significantly decrease to ~0.47 for both a-C:H and PLC films after annealed at 800°C. However, a-C:H films only indicate the decrease in S-parameters at shallower region of the films. These results suggest that a-C:H films are thermally more stable than PLC films.

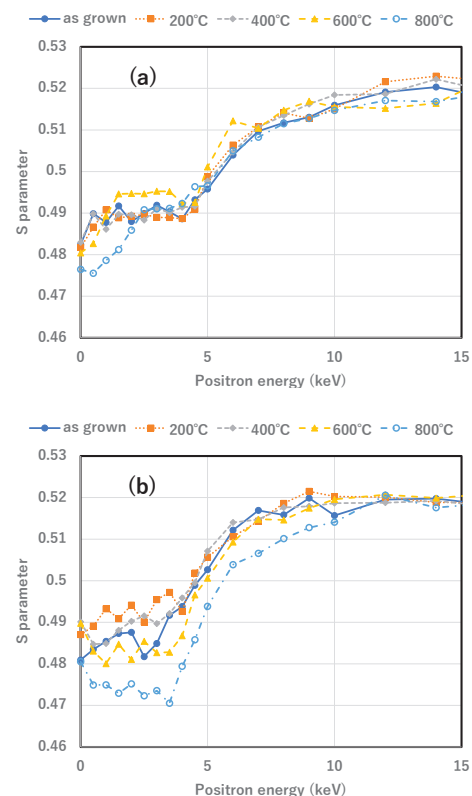


Fig. 1. The change in S-parameters against positron energy of (a) a-C:H and (b) PLC films at different annealing temperature.

REFERENCES:

- [1] S. Nakao et al., KURRI Progress Report 2016, 28P12-8 (2016) 57.
- [2] S. Nakao et al., KURRI Progress Report 2017, 29P6-8 (2017) 32.
- [3] S. Nakao et al., KURRI Progress Report 2018, 30P1-8 (2018) 11.
- [4] S. Nakao et al., KURRI Progress Report 2019, 31P12-7 (2019) 114.
- [5] S. Miyagawa *et al.*, Surf. Coat. Technol., **156** (2002) 322-327.